Deliverable

H2020 COMPET-05-2015 project
"Small Bodies: Near And Far (SBNAF)"

Topic: COMPET-05-2015 - Scientific exploitation of astrophysics, comets, and planetary data
Project Title: Small Bodies Near and Far (SBNAF)
Proposal No: 687378 - SBNAF - RIA
Duration: Apr 1, 2016 - Mar 31, 2019

WP	**WP6, Synergies from ground and space**
Del.No	**D6.8**
Title	**3D shape models for large MBAs**
Lead Beneficiary	UAM
Nature	Report
Dissemination Level	Public
Est. Del. Date	31 Dec. 2018
Version	2.0
Date	January 10, 2019
Authors	A. Marciniak, V. Alí-Lagoa, P. Bartczak, M. Butkiewicz-Bąk, E. Podlewska-Gaca, G. Dudziński, K. Dziadura

Objectives of WP: To combine observational data from space and ground, from remote, disk-integrated data and disk-resolved data from interplanetary missions to obtain (validated) high-quality model solutions for a wide range of applications: improvement of the scientific understanding, answering key questions for the reconstruction of minor body properties, calibration aspects, support for Gaia density determination, Hayabusa-2 target characterization and operational support, tools and methods for applications to large object samples.

Description of deliverable

3D shape model solutions scaled by stellar occultations and thermo-physical modelling, for volume determinations of Gaia mass targets.

1 Introduction and scope

We present here the 3D shape, spin, and size model solutions of large Main Belt asteroids with mass values expected from the Gaia mission. The aim is to provide for these bodies reliable volume determinations with realistic error bars, that combined in the future with masses from Gaia astrometry

will enable precise bulk density determinations, and mineralogical studies of our sample of targets. These targets are mostly large asteroids, with diameters above 100 km, as such considered to be largely intact remnants of planetesimals, which formed the planets or became deposited in the main asteroid belt. Constraining their bulk density, not influenced by substantial voids, and combining it with reflectance spectra will provide constraints of their material composition.

This deliverable bases on the work described in D 6.4 ("Gaia asteroid list") and D 3.4 ("Asteroid volume determination"). In D 6.4 the selection criteria for choosing targets from full list of ~140 Gaia mass asteroids have been described. In deliverable D 3.4, the final list of 21 SBNAF Gaia mass targets has been created basing on the amount and quality of lightcurves obtained for them in this project and available from the literature. In D 3.4 targets needing most data have been identified, and available stellar occultations have been listed, in addition to considerations of advantages and disadvantages of various types of shape model representations in the view of volume determinations.

2 Observing campaign

The observing campaign of SBNAF Gaia mass targets complemented their available photometric datasets, often providing valuable data from unique geometries, improving the existing model solutions by probing previously unobserved parts of the surface. In many cases new data led to updating the zero phases and sidereal period values, e.g. for better flux predictions, necessary in the calibration aspect (see D 4.6, "Selection of secondary asteroid calibrators").

This extensive observing campaign has been conducted in SBNAF project within WP5, mainly in La Sagra (IAA CSIC, Spain), Piszkéstető (Konkoly, Hungary), and by GaiaGOSA amateur observers, but also from Kepler Space Observatory, within our accepted proposals. Used instruments and their parameters are summarised in D 6.4. Our targets have been observed by Kepler in last but one Campaign 18, and these data will be used to update some of the presented here models in the final deliverable of WP4: D 4.5 "Final asteroid models". The campaign has been coordinated by AMU team (Poland), mainly in a form of monthly updates of the list of currently visible SBNAF targets most needing new lighcturves from given apparition, and its modifications once enough data were gathered. The details of the executed observing runs were updated by observers in the internal target webpage (`http://asteroidstnos.iaa.es`). Gathered photometric data needed careful reduction and analysis to identify problems like star passages, colour extinction, bad pixels or other instrumental effects (this work was mainly done by AMU team). Targets of slow rotation additionally required good coordination of observers in order to cover the whole lightcurve, and a new functionality visualising phase coverage has been added to GaiaGOSA service, following the solutions developed in a project focused exclusively on slow rotators (Marciniak et al. 2015).

Too noisy or erroneous data had to be removed, also literature data published as composite lightcurves needed separate treatment. The agreed data exchange format was ATL (developed for Asteroid Photometric Catalogue, Lagerkvist et al. 1987), while data for available shape models came in the lightcurve inversion format, where magnitudes are changed to flux values, and the information on the geometry is added.

SuperWASP asteroid archive (Grice et al. 2017), "discovered" by us during this project substantially improved the situation of limited geometries from which some of the targets were observed, providing many additional lightcurves. Good example here is asteroid 654 Zelinda, which if it was not for the SuperWASP archive, would only have data from a half of its orbital path, what would disable finding its unique spin and shape. However, quite often data from this source were burdened with large noise and needed careful vetting before they could be used in the modelling.

The optical data gathered here will be made publicly available upon publication of a paper in a refereed journal - the previously unpublished lightcurve data will be sent to CDS archive.

3 Spin and shape modelling. Quality assessment.

Taking as input the upgraded lightcurve datasets, the SAGE algorithm (Shaping Asteroids with Genetic Evolution, Bartczak & Dudziński 2018) was used to create spin and shape models. The modelling was performed on a new AMU cluster purchased within SBNAF project and took from 1 up to 3 days for each model. The process proved to be succesfull for all of the SBNAF Gaia mass targets from the final list of 16 targets with rich and varied enough datasets.

The models were stored and exchanged via the internal version of the ISAM service (Interactive Service for Asteroid Models). Their final versions are now available on the public version of ISAM (`http://isam.astro.amu.edu.pl`, Marciniak et al. 2012). This way the Milestone 11 named "Completion of volume determination for Gaia mass targets" has been reached.

Also, we applied here the quality assessment system sketched in D 6.7 and developed in Bartczak & Dudziński (submitted). The uncertainty of SAGE spin and shape solutions has been calculated here by multiple cloning the final models and randomly modifying the size and radial extent of their shape features. These clones were checked for the ability to simultaneously reproduce all the lightcurves within their uncertainties. This way, the scale-free dimensions with the most extreme, but still possible shape feature modifications have been calcultated, and then were translated to diameters in kilometers using occultation fitting (see next chapter).

Nonconvex shape models created here using SAGE algorithm can now be compared to shape solutions from other methods stored in DAMIT database (http://astro.troja.mff.cuni.cz/projects/asteroids3D, Ďurech et al. 2010). In some cases presented here spin and shape solutions are the first models for these bodies ever created. See the section on individual targets for details.

4 Scaling the models by stellar occultations

Unlike in the majority of works on spins and shape models of asteroids, where usually scale-free models are presented, here we put our shape models to absolute scale. Moreover, we do it using independently two methods: stellar occultation fitting and thermo-physical modelling, in order to verify the mutual agreement and the reliability of error bars.

Occultation technique explanation and predictions can be found in e.g. D 6.1, D 5.1 and D 3.3. Only the occultations stored in PDS database (Dunham et al. 2016) with at least three internally consistent chords have been used, as fitting instantenuous shape contours to events with less chords is burdened with too large uncertainties. Three chords also did not guarantee precise size determination, because of substantial uncertainties in timing of some events, or unfortunate spatial grouping of chords.

Final uncertainty in volume comes from effects of shape and occultation timing uncertainties, and is usually larger than in TPM, as thermal data are very sensitive to size of the body, but various shape features play lesser role there. On the other hand, knowledge of precise sidereal period and spin axis position is of vital importance for proper phasing the shape models in both TPM, and in occultation fitting. So if the good fit is obtained by both methods, it provides firm confirmation for the spin parameters used.

5 Brief description of thermo-physical model (TPM)

The TPM implementation we used is an update of that in Alí-Lagoa et al. (2014), in turn based on Delbo' & Harris (2002). For the colour correction, however, we now use the H and G values tabulated in the JPL Horizons database to estimate an effective temperature considering the distance to the sun at the moment of the observation (see also deliverable D2.4). The heat diffusion is approximated as a one-dimensional problem and we apply the Lagerros approximation (Lagerros 1996, 1998; Müller & Lagerros 1998; Müller 2002). We also simplify the spectral emissivity to be constant with wavelength and equal to 0.9 (see, e.g. Delbo' et al. 2015). The Bond albedo, another necessary input for the TPM, consisted of an average value based on the different radiometric diameters available from AKARI and/or WISE, and all available H-G, H-G_{12}, and H-G_1-G_2 values from the Minor Planet Center, Oszkiewicz et al. (2011), or Vereš et al. (2015). With all these assumptions, we have two free parameters, the scale of the shape (usually called the diameter, D) and the thermal inertia (Γ). We explored different roughness parametrisations by varying the opening angle of hemispherical craters covering 0.6 of the area of the facets (following Lagerros 1996). The diameters and other relevant information related to the TPM analyses of our targets are provided in Table 2. Whenever the data are too few to provide realistic error bar estimates, we report the best-fitting diameter so that the models can be scaled and compared to the scaling given by the occultations.

On the other hand, if we have multiple good-quality thermal data (with absolute flux errors below 10%) then this typically translates to a size accuracy of around 5% (at least if the shape is not too extreme and if the spin vector is known reasonably well). This rule-of-thumb certainly works for the large MBAs, i.e. the Gaia mass sample.

6 Individual targets

6.1 (3) Juno

Lightcurves from 8 apparitions were used to construct SAGE model of Juno. They displayed small amplitudes of brightness variations: from 0.12 to 0.22 mag, indicating small elongation of this body. SAGE model can be compared with the model made with ADAM method by (Viikinkoski et al. 2015), based on ALMA and adaptive optics data in addition to the same set of lightcurves. Both models fit the visual lightcurves at similarly good level. As can be seen in Fig. 1 the polar crater has been reproduced on both shapes, but other shape features are different. Apparently the available set of lightcurves did not contain enough information for such detailed shape models as the one complemented with auxiliary data. It is worth noting however, that spin period and axis position agree almost perfectly between the two model solutions.

Three stellar occultation have been used to scale the SAGE model in kilometers: from the years 1979, 2000, and 2014, with the most densely covered one from 1979. The fit of 2D shape projections to these chords is not perfect, misfitting some features suggested by the chords, however their mutual inconsistence can also be partially to blame.

Another indication of imperfectness of the SAGE shape model is that sphere with the same rotation parameters fits thermal data better, where especially rich dataset was available, containing 112 infrared measurements. Still, the sizes from both occultation fitting (236 - 260 km, tab 1) and thermo-physical modelling (254 km, tab 2) of this solution agree with ADAM-based size (248 ± 5) within the error bars. All sizes given in this work are the diameters of equivalent volume spheres.

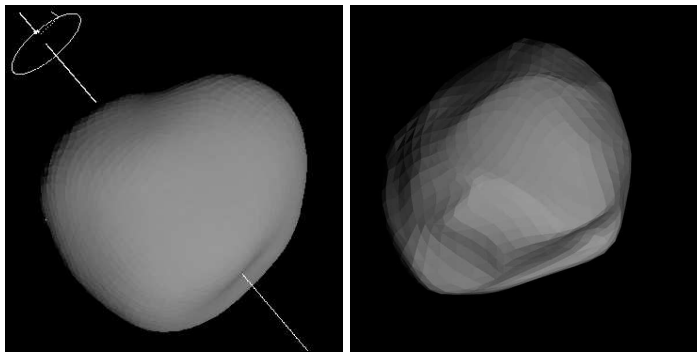

Figure 1: Sky projections for the same epoch of SAGE (left) and ADAM (right) shape models of asteroid (3) Juno. Both shapes contain a crater near the south pole, but differ otherwise.

6.2 (13) Egeria

We had lightcurves for Egeria from 8 apparitions, not optimally spaced on its orbit though. Their character was asymmetric, with minima of various depths, while lightcurve amplitudes ranged from 0.12 to 0.37 mag. SAGE highly irregular shape model with large polar crater fits them with some notable problems, lesser though than in convex model by (Hanuš et al. 2011), but larger than in ADAM solution from (Hanuš et al. 2017). SAGE spin solution agrees wih the latter only in the spin axis longitude, while the sidereal period and the pole latitude disagree, so probably the SAGE solution drifted to some local minimum instead of the global one.

There were two multi-chord stellar occultations available for Egeria; from 2008 from 2013. The fit of shape model projection to the latter is good, but the one from 2008 was not fitted properly by neither of the mirror pole solutions, where SAGE shape displays lesser elongation than the corresponding ADAM solution.

The imperfections of SAGE shape model is also reflected by the large range of diameters possible from occultation fitting: from 193 to 294 km, surpassing their error bars (see table 1), but also by problems in fitting IRAS data in thermo-physical modelling. The spherical shape approximations with the same spin parameters provides fit to thermal data on a similar level, however there were no thermal lightcurves available (table 2). The diameter from thermal data is around 200 km, but no realistic error bars can be determined.

6.3 (14) Irene

Lightcurves of Irene were also asymmetric (amplitude from 0.03 to 0.16 mag) and changed character from bimodal to monomodal in some apparitions, indicating low inclination of the spin axis. They were gathered during as many as 12 apparitions, somewhat grouped in sky longitude. SAGE model fits them very well, close to the noise level.

The fit of this model to only three chord occultation revealed preferred spin solution, in agreement with the only solution found by Viikinkoski et al. (2017) using ADAM algorithm and adaptive optics images in addition to lightcurves. The size of SAGE model from occultation fitting (145 km) agrees with size from TPM (155 km) within the error bars, however there were too few thermal data for their realistic estimation in TPM. Both size determinations also agree with the size of ADAM shape model scaled using Adaptive Optics imaging (153 km ± 6km). SAGE shape model based on less sophisticated techniques (pure lightcurve inversion from point-like source observations) is

also in a very good agreement with ADAM model, displaying the same major shape features as that model (see Fig. 2). This agreement can be checked for all available models by generating their sky projections on the same moment in ISAM[1] and DAMIT[2] webpages.

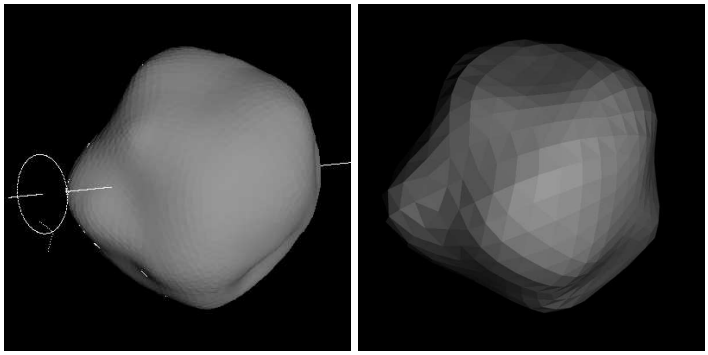

Figure 2: Sky projections for the same epoch of SAGE (left) and ADAM (right) shape models of asteroid (14) Irene. Both shapes are in very good agreement.

6.4 (20) Massalia

Data from 13 apparitions were at our disposal, but again some of the apparitions grouped in one place in the orbit. Massalia displayed rather regular, bimodal lightcurves of amplitudes from 0.17 to 0.27 mag. The fit of SAGE model synthetic lightcurves to majority of the these lightcurves is very good, with some misfits in a few consecutive ones, indicating possible systematics in that data.

The crude shape model from Kaasalainen et al. (2002) has been improved by Hanuš et al. (2016), however the latter is not available at DAMIT. So SAGE model definitely improves the available one, providing smooth shape, with somewhat rhomboidal appearance. The spin parameters agree with the values by Hanuš et al. (2016), confirming that initial solution by Kaasalainen et al. (2002) was off, with its much lower pole inclination and sidereal period differing by 0.002 hours, which is actually a large mismatch considering the shortness of the period and long span (60 years) of the photometric dataset. Such a difference would result in large shift in phase after the huge number of rotations along this time span.

The fit of SAGE shape projection to the only occultation event from 2012 is acceptable, however the resulting size (106 and 133 km depending on the pole solution) is substantially smaller than the one from TPM (145 km), and the disagreement is outside both error bars combined (see tables 1 and 2). On the other hand, SAGE shape fitted to thermal data much better than a sphere, so it should be close to real shape of Massalia. The underestimated size from fitting to occultation chords was probably caused by their unfortunate spatial grouping or small phasing problems of the model.

6.5 (64) Angelina

Angelina displayed strongly asymmetric and variable lightcurves, with amplitudes ranging from as small as 0.04 mag to as large as 0.42 mag, a strong indicator of low pole inclination. Data from 10 apparitions were used to create its SAGE model and were fitted by it at a good level. Indeed, the

[1] http://isam.astro.amu.edu.pl

[2] http://astro.troja.mff.cuni.cz/projects/asteroids3D

pole was found at low values of latitude, consistent with previous solution by Ďurech et al. (2011). However SAGE solution differs from it in the period value, at a substantial level of 0.0015 hours. It is worth noting, that crude convex solution by Ďurech et al. (2011) was based on dense lightcurves from only three apparitions, complemented by sparse data of the uncertainty of 0.1 - 0.2 mag, so at the level of lightcurve amplitude of this target. Richer and better quality dataset used for SAGE model are in favour for the latter. Also, the level of the occultation fit point to smoothly shaped SAGE model as a better solution.

This model also worked well with the thermal data, providing sizes slightly larger, but consistent with the ones from occultation fitting (54 vs. 50 km, see tables 1 and 2). TPM also pointed to preferred pole solution from two mirror pole solutions which are usual outcome of lightcurve inversion methods.

6.6 (68) Leto

For Leto, data from six different apparitions consisted of somewhat asymmetric lightcurves, with unequally spaced minima. Amplitudes ranged from 0.10 to 0.28 mag. Angular convex shape model published previously by Hanuš et al. (2013), basing mainly on sparse data was superseded here by much smoother SAGE model. Their on-sky projections on the same epoch can be compared in Fig. 3.

The fit to the lightcurves is mostly good, better in the first pole solution. There was only one 3-chord occultation, and the model fits to it imperfectly, and again one of the poles seems to be preferred (pole 2 this time). TPM resulted in almost the same level of fit for both poles, with similar sizes. However the size for pole 1 solution from occultation fitting is 20 km larger that that from TPM (152 vs. 121 km), with similarly large error bars. The second pole solution displays here smaller uncertainties, and size (133 km) more consistent with TPM best solution.

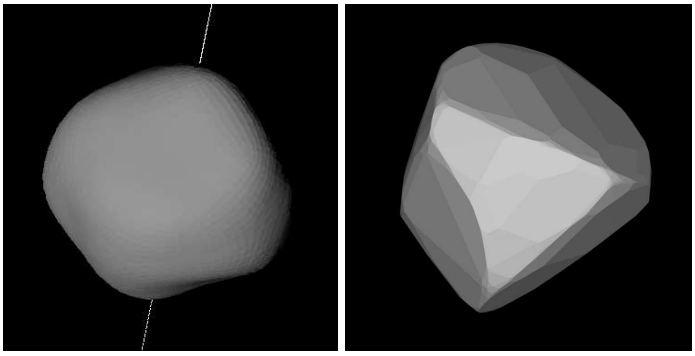

Figure 3: Sky projections for the same epoch of SAGE (left) and convex inversion (right) shape models of asteroid (68) Leto. SAGE provided largely different and much smoother shape solution.

6.7 (89) Julia

Asteroid Julia was added to our list of targets because of sharing this target with VLT large programme 199.C-0074 (PI: Pierre Vernazza). In this programme a rich set of well resolved adaptive optics images have been obtained using VLT/SPHERE instrument. Spin and shape modelling has been performed using ADAM algorithm on lightcurves and AO images, what enabled to reproduce

major nonconvex shape features of this target (Vernazza et al. 2018). In this work a large impact crater has been identified on the surface, as a possible source region of asteroids from Julia family. However SAGE model, basing only on disk-integrated photometry, also reproduced the biggest crater and some of the hills present in ADAM model (Fig. 4).

Interestingly, for both models data from only four apparitions were used. One of them however spanned as many as five months, covering large range of phase angles, that due to various levels of shadowing highlighted the surface features. Both models fit them similarly well, SAGE model slightly worse. Spin parameters agree to a very good level. In the occultation fitting (to two multichord events from the years 2005 and 2006) some of the SAGE shape features seem too small, and others too large, but overall it gives size (138 km) consistent with ADAM model size (139 ± 3 km). This model applied with the thermal data in TPM provides slightly larger size (150 km), but consistent within the error bars. It should be noted that thermal data were unevenly distributed on Julia's surface, covering only northern hemisphere of this body.

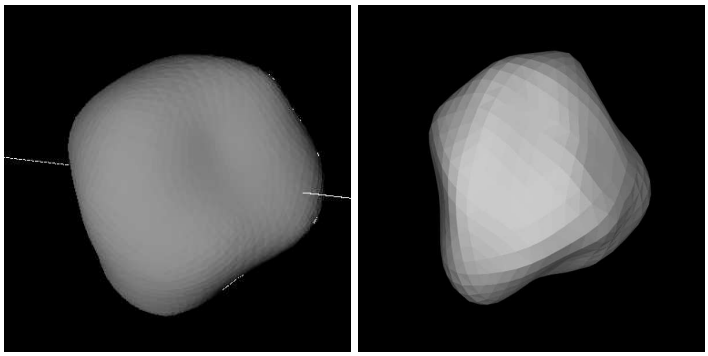

Figure 4: Sky projections for the same epoch of SAGE (left) and ADAM (right) shape models of asteroid (89) Julia. Similar crater has been reproduced by both methods.

6.8 (114) Kassandra

Lightcurves of Kassandra form 9 apparitions (but only 6 distinct geometries) showed sharp minima of uneven depths and had amplitudes from 0.15 to 0.25 mag. SAGE shape model based on them looks quite irregular, with deep polar crater. It does not resemble convex model by Ďurech et al. (2018b), which is however provided with a warning of its wrong inertia tensor. Still, the spin parameters of both solutions roughly agree. SAGE model fits the lightcurves well, except for three cases, the same ones which convex model also had problems fitting. This might indicate that they are burdened with some instrumental or other systematic errors.

Unfortunately there are no well covered stellar occultations available for Kassandra, so the only size determination could be done here by TPM (see table 2). In spite of substantial irregularity of SAGE shape model, the spherical shape gives similarly good fit to thermal data.

6.9 (145) Adeona

In spite of the fact that available to us set of lightcurves came from 9 apparitions, their unfortunate grouping resulted in only 5 distinct viewing aspects of this body. Very small amplitudes (0.04 - 0.15 mag) displayed by this target were additional hindering factor, so much that initially there was

a controversy whether its period is close to 8.3 or 15 hours. It was resolved by good quality data obtained by Pilcher (2010), in favour of the latter. SAGE model fitted most of the lightcurves well, but had problems with some, where visible misfit is notable.

This is the first model of this target, so there is no previous model to compare with. SAGE model looks almost spherical, without notable shape features, so as expected the spherical shape provided similarly good fit to thermal data. The only available stellar occultation had strongly grouped chords, that lead to unrealistically high size estimate (see tab 1) with extremely large error bars. The situation is somewhat better for the miror pole solution, which size (178 km) is roughly consistent with diameter from TPM (145 km) taking into account its large error bars.

6.10 (297) Caecilia

There were data from 9 apparitions available for Caecilia, well spread in ecliptic longitude. The lightcurves displayed mostly regular, bimodal character of 0.15 - 0.28 mag amplitudes. Previous model by Hanuš et al. (2013) was created on much poorer dataset, with dense lightcurves from only 1/3 of the orbit, supplemented by sparse data. So as expected, that shape model is rather crude, as compared to SAGE model. Both models had similar problems fitting some of the lightcurves. Spin period and pole agree well between the two models.

There is no stellar occultation by Caecilia available with sufficient number of chords, so SAGE model has been scaled here only by TPM (see table 2). However the diameter has been estimated here only tentatively, as the uncertainty cannot be determined due to very small number of thermal measurements.

6.11 (308) Polyxo

Available lightcurve dataset has been very limited for Polyxo, so no model could have been constructed, but thanks to extensive SBNAF observing campaign we now have data from 6 apparitions covering 5 different aspects. Lightcurves of this target were very irregular and had small amplitude (0.08-0.22 mag), often displaying three maxima per period, which is quite unusual. However, SAGE shape model looks rather smooth, with only small irregularities. Its fit to visible lightcurves is mostly good.

There were three multi-chord occultations for Polyxo in PDS, from the years: 2000, 2004, and 2010. Obtained shape models for both of the pole solutions fit them at good level, which is confirmed by mutual consistence of diameters separately derived from each of the events (125-133 km, see table 1). TPM diameter (139 km) is slightly larger though, but again too few thermal data disabled the calculation of realistic error bars here. Probably also for this reason a spherical shape approximation fits thermal data better.

6.12 (381) Myrrha

In the case of Myrrha there were data from 7 apparitions, but 5 different viewing aspects. The lightcurves were regular, with large, 0.30 - 0.36 mag amplitudes. Silarly to Caecilia, without SBNAF data the viewing geometries have been limited to 1/3 of Myrrha orbit. So previous model by Hanuš et al. (2016) had to be constructed on dense lightcurves supplemented with sparse data, and looks somewhat angular (see comparison of both shapes in fig. 5). Due to very high inclination of the pole (spin axis points far away from the ecliptic plane), only one solution for the pole position

has been obtained, and it agrees with the previous model. Fit of both models to the lightcurves is good.

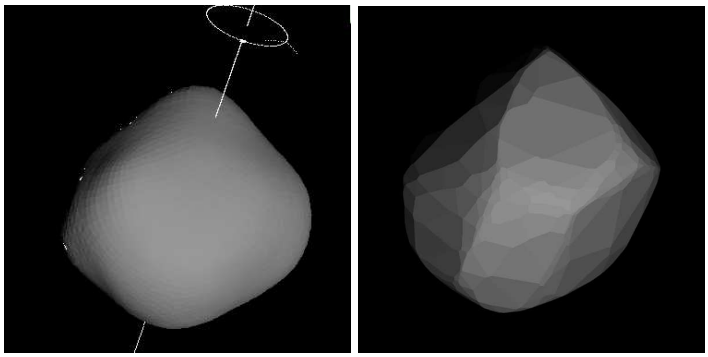

Figure 5: Sky projections for the same epoch of SAGE (left) and convex inversion (right) shape models of asteroid (381) Myrrha. SAGE model is similar to the one from convex inversion, but provides better resolution.

There was a very densely covered stellar ocultation by Myrrha available, however some of 25 chords are mutually inconsistent and burdened with large uncertainties. The diameter of the best fitting model size is 135 km, with error bars enlarged by inaccurate timing of some of the events (tab. 1). In the thermal aspect SAGE model of Myrrha fits the rich dataset much better than a corresponding sphere, resulting in precisely determined size (131 ± 4 km), in close agreement with size derived from the occultation fitting.

6.13 (402) Chloe

A different case is Chloe, where data from 9 apparitions were available, but they were grouped in three places in its orbit. Chloe usually displayed rare, monomodal lightcurve character, with only one deep minimum, and the amplitudes ranging from 0.19 to 0.37 mag. The shape model by Hanuš et al. (2016) based on sparse and dense data notably misfits most of the lighturves in amplitude, but agrees with SAGE model in spin parameters: the period and spin axis position.

However SAGE shape model also has problems fitting many of the lightcurves, and looks quite extreme. It contains deep indentations and steep hills, unusual shape features for such a large body (D~53 km). Unfortunately there is no good stellar occultation to confirm or reject this shape model. In TPM it fits badly, and residuals connected with phase are correlated for various missions, indicating problems with the shape model. Photometric data from other geometries would be needed to improve it.

6.14 (441) Bathilde

There were data from 10 apparitions covering 7 viewing geometries at our disposal. Lightcurves of Bathilde were mostly regular, sometimes with minima differing by depth, and amplitudes ranging form 0.08 to 0.22 mag. Similarly as in a few already described cases, previous model of this target based on sparse and dense data was available (Hanuš et al. 2013), with crude shape representation. SAGE model agrees with it in spin parameters and goodness of the fit to the lightcurves, but due to richer and denser dataset, the shape model is smoother.

Shapes for both SAGE pole solutions fit the only available occultation well, and the resulting size (~77 km) agrees with the size from TPM (72 km), but due to unfortunate distribution and length of all four chords, the size could be even twice as big and still fit them (see table 1). Interestingly, the second solution for the pole seems to be rejected by TPM, and the favoured one fits thermal data much better than a corresponding sphere.

6.15 (654) Zelinda

Due to a very long rotation period of Zelinda (almost 32 hours), there were not many full lightcurves available previously, and consequently, also no spin and shape model. SBNAF observing campaign combined with data mining of the SuperWASP archive (Grice et al. 2017), resulted in obtaining rich and varied enough dataset (6 aspects), enabling to construct unique SAGE model. In addition to slow rotation Zelinda also displayed small lightcurve amplitudes: 0.08 to 0.26 mag.

The shape model, as expected from lightcurve character, shows small elongation and a smooth shape. There were three stellar occultations that could be used to scale it: from the years 2012, 2013, and 2015. The fit was mostly good, and resulting diameters ranged from 98 to 123 km. Exactly the same value as the latter was obtained when applying this shape model in TPM, moreover, pole 2 solution could be rejected (see table 2).

6.16 (704) Interamnia

This is an interesting case, where in spite of rich photometric dataset available, only an ellipsoidal approximation of the shape has been done previously (Michalowski et al. 1995). Its extremely small amplitudes (0.04 - 0.17 mag) coming from geometries limited to only a half of its orbital path are to blame. In SBNAF project we added data from the year 2016 and 2017 which improved the situation, and enlarged the number of available apparitions to nine. SAGE shape model of Interamnia looks quite round, and the shape solution, as often happens when verifying the ellipsoidal shape models, turned out to be completely different: a retrograde sense of rotation instead of prograde, with sidereal period shorter by as much as 0.015 hours. However, SAGE model had problems fitting some of the lightcurves.

Interamnia is also interesting target due to wealth of multi-chord occultations (five, with one counting as many as 46 chords), and thermal measurements (103). Still, the fit to occultations is visibly imperfect, with pole 2 solution fitting somewhat better than pole 1. Sizes obtained this way ranged from 295 to 347 km. In TPM both solutions fitted thermal data on a similar lever, only slightly better that a sphere though. As a result only its size is well determined: 334 ± 4 km, closer to the larger of the sizes from occultations (tab 1).

6.17 (721) Tabora

After the SBNAF observing campaign in all we had data from 5 apparitions for Tabora. Amplitudes ranged from 0.19 to 0.50 mag, and the lightcurves sometimes were strongly asymmetric, with extrema at different levels. There is a recently published model of Tabora, based on joining sparse data in the visible with WISE thermal data (bands W3 and W4, Ďurech et al. 2018a). The resulting shape model is somewhat angular, but is in agreement with SAGE model with respect to spin parameters. SAGE model is also rather extreme, with some probable artifacts.

Stellar occultations are lacking for Tabora, but TPM gave borderline acceptable fit in case of pole 1, which works with thermal data substantially better than a sphere. See table 2 for size estimate.

7 Conclusions

In D 6.1 ("Occultation vs. thermal tools") the strengths and limitations of both techniques have been studied, and the conclusion was that in many ways they are complementary to each other. The results obtained here support this fact. Occultation fitting, where it was possible, enabled to confirm major shape features and spin parameters of SAGE shape models, providing rough diameters, while thermo-physical modelling resulted in more precise diameters, additionally constraining thermal parameters: thermal inertia and surface roughness. The diameters based on occultation fitting of complex shape models, inaccurate as they may seem here compared to those from TPM, still reflect the dimensions of real body better than commonly used elliptical approximation of the shape projection. The biggest advantage of scaling 3D shape models by occultations is that this procedure provides volumes of these bodies, unlike the fitting of 2D elliptical shape approximations, that only provides the lower limit for the size of the projection ellipse.

Diameters determined here can be easily translated to volumes following the equation:

$$V = \frac{\pi(D)^3}{6}. \tag{1}$$

Resulting volumes, especially those with relatively small uncertainty, are going to be a valuable input for density determinations of these targets once the mass values from Gaia mission astrometry become available. In the cases where only convex solutions were previously available, nonconvex solutions created here will lead to more precise volumes, and consequently better constrained densities.

Constructed here shape models, spin parameters, diameters and volumes from occultation fitting and thermo-physical modelling are now available on the public ISAM webpage, together with accompanying uncertainties.

Table 1: Results from the occultation fitting of SAGE models. Mirror pole solutions are coded "pole 1" and "pole 2". Third column gives the dimensionless volume, with R=1 being the radial distance of the farthest point from the center of mass. Scaled sizes are given in kilometres as the diameters of equivalent volume spheres.

Number	Name	pole	Volume (R=1)	Year of occultation	Diameter (km)	$+\sigma D$	$-\sigma D$
3	Juno		2.44528797200E+00	1979-12-11	259.6	12.9	-11.7
			2.44528797200E+00	2000-05-24	236.0	19.7	-16.9
			2.44528797200E+00	2014-11-20	249.7	11.9	-10.9
13	Egeria	1	2.03081958000E+00	2008-01-22	219.3	18.1	-15.6
			2.03081958000E+00	2013-03-26	215.6	15.4	-16.5
		2	2.19133140344E+00	2008-01-22	193.9	11.9	-11.9
			2.19133140344E+00	2013-03-26	294.4	6.6	-6.4
14	Irene	1	2.77004181490E+00	2013-08-02	145.8	12.0	-11.5
		2	2.68328737990E+00	2013-08-02	145.2	91.5	-18.1
20	Massalia	1	2.31087993400E+00	2012-10-09	106.5	4.8	-2.8
		2	2.63821470940E+00	2012-10-09	113.5	6.2	-9.9
64	Angelina	1	1.90904638610E+00	2004-07-03	48.9	3.8	-2.3
		2	1.84373537200E+00	2004-07-03	50.7	2.1	-3.0
89	Julia		2.69739017400E+00	2005-08-13	138.7	14.2	-6.4
			2.69739017400E+00	2006-12-04	137.3	2.1	-4.5
68	Leto	1	2,48214075000E+00	1999-05-23	152,0	20,8	-18,3
		2	2.29882540000E+00	1999-05-23	132.8	8.4	-8.0
145	Adeona	1	3.32233438400E+00	2005-02-02	627.6	608.7	-465.6
		2	3.19502850600E+00	2005-02-02	178.0	51.3	-34.5
308	Polyxo	1	2.86181722780E+00	2000-01-10	133.5	5.8	-6.3
			2.86181722780E+00	2004-11-16	125.4	11.1	-8.6
			2.86181722780E+00	2010-06-02	128.8	3.0	-2.8
		2	2.71617722400E+00	2000-01-10	131.2	5.0	-2.9
			2.71617722400E+00	2004-11-16	125.3	10.7	-8.1
			2.71617722400E+00	2010-06-02	127.8	3.5	-4.3
381	Myrrha		2.24435686000E+00	1991-01-13	134.8	45.3	-12.8
441	Bathilde	1	2.53797145140E+00	2003-01-11	75.3	74.6	-10.0
		2	2.35878434150E+00	2003-01-11	76.8	15.9	-9.1

Table 1: contd.

Number	Name	pole	Volume (R=1)	Year of occultation	Diameter (km)	$+\sigma D$	$-\sigma D$
654	Zelinda	1	2.90046195440E+00	2012-01-06	99.6	8.8	-8.1
			2.90046195440E+00	2013-05-12	119.1	0.5	-0.5
			2.90046195440E+00	2015-12-31	110.4	4.8	-5.8
		2	2.75424240480E+00	2012-01-06	97.6	4.9	-3.0
			2.75424240480E+00	2013-05-12	113.9	6.3	-4.0
			2.75424240480E+00	2015-12-31	123.0	3.3	-5.0
704	Interamnia	1	3.52175997800E+00	1996-12-17	325.4	33.8	-19.3
			3.52175997800E+00	2003-03-23	315.8	0.0	-9.2
			3.52175997800E+00	2007-09-09	342.6	0.0	-3.8
			3.52175997800E+00	2009-01-11	335.8	7.4	-3.6
			3.52175997800E+00	2012-11-12	331.8	7.2	-23.0
		2	3.43915197380E+00	1996-12-17	322.9	25.5	-19.1
			3.43915197380E+00	2003-03-23	323.1	0.0	-6.6
			3.43915197380E+00	2007-09-09	347.4	0.0	-3.9
			3.43915197380E+00	2009-01-11	295.1	0.0	0.0
			3.43915197380E+00	2012-11-12	332.8	0.0	-10.5

Table 2: Summary of TPM results, including the minimum reduced chi-squared ($\bar{\chi}^2_m$), the best-fitting diameter (D) and corresponding 1σ statistical error bars, and the number of IR data modelled ($N_{\rm IR}$). TLC (Yes/No) refers to the availability of at least one thermal light curve with eigth or more points sampling the rotation period. The $\bar{\chi}^2_m$ obtained for a spherical model with the same spin properties is also shown. Whenever the two mirror solutions provided different optimum diameters, we show them in different lines. Acceptable solutions (and preferred ones whenever it applies to mirror models) are highlighted in bold face.

Target [pole]	$N_{\rm IR}$	TLC	$\bar{\chi}^2_m$	$D \pm \sigma D$ (km)	$\bar{\chi}^2_m$ for sphere	Comments
(3) Juno	112	No	1.3	254 ± 4	1.0	Borderline acceptable fit. Sphere does better
(13) Egeria 1	12	No	0.80	200	0.9	IRAS data not fitted. Unrealistically high Γ
(13) Egeria 2	12	No	0.80	196	0.8	IRAS data not fitted. High Γ fits better
(14) Irene 1	6	No	0.1	155	0.4	Very few data to provide realistic error bars
(14) Irene 2	6	No	0.2	154	0.2	*Idem*
(20) Massalia 1,2	72	No	0.5	145±2	1.6	Mirror solutions provide virtually same fit
(64) Angelina 1	23	Yes	0.8	54 ±2	1.10	Did not model MSX data
(64) Angelina 2	23	Yes	1.16	54 ±2	1.24	*Idem*
(68) Leto 1	55	Yes	0.6	121 ± 5	0.83	Small offset between mirror solutions (not stat. significant)
(68) Leto 2	55	Yes	0.7	123 ± 5	0.87	*Idem*
(89) Julia	27	No	1.0	150 ± 10	1.5	Only northern aspect angles covered ($A < 70$ deg) in the IR. Unexpectedly high thermal inertia fits better
(114) Kassandra 1,2	46	Yes	0.6	98 ± 3	0.70	Quite irregular but spheres provide similar fit
(145) Adeona 1,2	17	No	0.25	145	0.23	Too few data to give realistic error bars
(297) Caecilia	13	No	0.9	41	0.9	Too few data to give realistic error bars
(308) Polyxo 1,2	13	No	0.4	139	0.35	Too few data to give realistic error bars
(381) Myrrha	73	Yes	0.40	131±4	1.6	Good fit but some small waviness in residuals vs. rot. phase plot
(402) Chloe 1	33	Yes	1.6	51	1.8	Bad fit. Residuals vs. phase correlated for different missions
(402) Chloe 2	33	Yes	1.5	53	1.8	Borderline bad fit. Residuals vs. phase correlated
(441) Bathilde 1	26	Yes	0.7	72 ± 2	1.7	Very high thermal inertia
(441) Bathilde 2	26	Yes	1.6	–	> 2	Bad fit
(654) Zelinda 1	41	No	0.7	123±5	1.5	Removed 2 IRAS outliers
(654) Zelinda 2	41	No	1.3	122±6	> 2	Borderline acceptable fit. Removed 2 IRAS outliers
(704) Interamnia 1,2	103	No	0.8	334±4	1.0	
(721) Tabora 1	40	Yes	1.4	78±5	> 5	Borderline acceptable fit, still better than sphere
(721) Tabora 2	40	Yes	2.1	–	> 5	Bad fit

References

Alí-Lagoa, V., Lionni, L., Delbo, M., et al. 2014, A&A, 561, A45

Bartczak, P. & Dudziński, G. 2018, MNRAS, 473, 5050

Delbo', M. & Harris, A. W. 2002, Meteoritics and Planetary Science, 37, 1929

Delbo, M., Mueller, M., Emery, J. P., Rozitis, B., & Capria, M. T. 2015, Asteroid Thermophysical Modeling, ed. P. Michel, F. E. DeMeo, & W. F. Bottke, 107–128

Dunham, D. W., Herald, D., Frappa, E., et al. 2016, NASA Planetary Data System, 243, EAR

Ďurech, J., Hanuš, J., & Alí-Lagoa, V. 2018a, A&A, 617, A57

Ďurech, J., Hanuš, J., Brož, M., et al. 2018b, Icarus, 304, 101

Ďurech, J., Kaasalainen, M., Herald, D., et al. 2011, Icarus, 214, 652

Ďurech, J., Sidorin, V., & Kaasalainen, M. 2010, A&A, 513, A46

Hanuš, J., Ďurech, J., Brož, M., et al. 2013, A&A, 551, A67

Hanuš, J., Ďurech, J., Brož, M., et al. 2011, A&A, 530, A134

Hanuš, J., Ďurech, J., Oszkiewicz, D. A., et al. 2016, A&A, 586, A108

Hanuš, J., Viikinkoski, M., Marchis, F., et al. 2017, A&A, 601, A114

Kaasalainen, M., Torppa, J., & Piironen, J. 2002, Icarus, 159, 369

Lagerkvist, C.-I., Barucci, M. A., Capria, M. T., et al. 1987, Asteroid photometric catalogue.

Lagerros, J. S. V. 1996, A&A, 310, 1011

Lagerros, J. S. V. 1998, A&A, 332, 1123

Marciniak, A., Bartczak, P., Santana-Ros, T., et al. 2012, A&A, 545, A131

Marciniak, A., Pilcher, F., Oszkiewicz, D., et al. 2015, Planet. Space Sci., 118, 256

Michalowski, T., Velichko, F. P., Di Martino, M., et al. 1995, Icarus, 118, 292

Müller, T. G. 2002, Meteoritics and Planetary Science, 37, 1919

Müller, T. G. & Lagerros, J. S. V. 1998, A&A, 338, 340

Oszkiewicz, D. A., Muinonen, K., Bowell, E., et al. 2011, J. Quant. Spec. Radiat. Transf., 112, 1919

Pilcher, F. 2010, Minor Planet Bulletin, 37, 148

Vereš, P., Jedicke, R., Fitzsimmons, A., et al. 2015, Icarus, 261, 34

Vernazza, P., Brož, M., Drouard, A., et al. 2018, A&A, 618, A154

Viikinkoski, M., Hanuš, J., Kaasalainen, M., Marchis, F., & Ďurech, J. 2017, A&A, 607, A117

Viikinkoski, M., Kaasalainen, M., Ďurech, J., et al. 2015, A&A, 581, L3